Adv Comput Math (2018) 44:87–114
DOI 10.1007/s10444-017-9536-x

A linear formulation for disk conformal parameterization of simply-connected open surfaces

Gary Pui-Tung Choi[1] · **Lok Ming Lui**[2]

Received: 1 August 2016 / Accepted: 5 April 2017/
Published online: 20 April 2017

Abstract Surface parameterization is widely used in computer graphics and geometry processing. It simplifies challenging tasks such as surface registrations, morphing, remeshing and texture mapping. In this paper, we present an efficient algorithm for computing the disk conformal parameterization of simply-connected open surfaces. A double covering technique is used to turn a simply-connected open surface into a genus-0 closed surface, and then a fast algorithm for parameterization of genus-0 closed surfaces can be applied. The symmetry of the double covered surface preserves the efficiency of the computation. A planar parameterization can then be obtained with the aid of a Möbius transformation and the stereographic projection. After that, a normalization step is applied to guarantee the circular boundary. Finally, we achieve a bijective disk conformal parameterization by a composition of quasi-conformal mappings. Experimental results demonstrate a significant improvement in the computational time by over 60%. At the same time, our proposed method retains comparable accuracy, bijectivity and robustness when compared with the state-of-the-art approaches. Applications to texture mapping are presented for illustrating the effectiveness of our proposed algorithm.

Communicated by: Yang Wang

✉ Lok Ming Lui
lmlui@math.cuhk.edu.hk

Gary Pui-Tung Choi
pchoi@g.harvard.edu

[1] John A. Paulson School of Engineering and Applied Sciences, Harvard University, Cambridge, MA, USA

[2] Department of Mathematics, The Chinese University of Hong Kong, Hong Kong, Hong Kong

Keywords Disk conformal parameterization · Simply-connected open surface · Quasi-conformal theory

Mathematics Subject Classification (2010) 37K25 · 68U05 · 68U10

1 Introduction

With the advancement of computer technologies and 3D acquisition techniques, 3D objects nowadays are usually captured and modeled by triangular meshes for further usages. A large number of applications of triangular meshes can be found in computer graphics and computer-aided design. However, working on general meshes is a difficult task because of their complicated geometry. The complicated geometry hinders applications such as surface registration, morphing and texture mapping. To overcome this problem, one common approach is to parameterize the surfaces onto a simple parameter domain so as to simplify the computations. For instance, textures can be designed on the simple domain and then mapped back onto the original surfaces [17, 25, 51]. Another example that usually makes use of parameterization is surface registration [3, 16, 26–29, 31, 32, 36–38]. Instead of directly computing the registration between two convoluted surfaces, one can perform the registration on the simple parameter domain, which is much easier. It is also common to perform surface remeshing with the aid of parameterizations [19, 42, 43]. With the development of the computer industry, the problem of finding a good parameterization method is becoming increasingly important.

To make a parameterization useful and applicable, one should seek for a method that minimizes certain types of distortions. In particular, it is desirable to minimize the angular distortions of the 3D meshes. For instance, with the angular distortions minimized, regular triangle elements on high-quality meshes will remain to be regular on the parameter domain. The preservation of the high quality of meshes is important for solving geometric PDEs [7, 30]. *Angle preserving parameterizations*, also known as *conformal parameterizations*, effectively preserve the local geometry of the surfaces. Hence, in this paper, our goal is to develop an efficient conformal parameterization algorithm.

The choice of the parameter domain is also a key factor in deciding the parameterization scheme for simply-connected open surfaces. In many practical applications, enforcing the parameter domain to be a regular shape, such as the unit disk, is preferred over having an arbitrary shape. For instance, in surface remeshing, one common approach is to flatten a mesh onto the plane and then perform the remeshing procedure by building a new simple mesh structure on the planar domain. The remeshing procedure on a circular domain is much easier than that on an arbitrary domain. Specifically, the circular domain is always convex while other arbitrary domains may be non-convex and hence existing meshing schemes, such as the Delaunay triangulation method, may produce unwanted elements outside the domains. Also, the disk conformal parameterization is more useful than free-boundary parameterization in solving PDEs on meshes. For example, the Poisson's equation has exact form solutions on disk domain but not necessarily on other arbitrary domains. The

solutions on the disk parameterizations can then be used to obtain the solutions on the original meshes. Besides, the disk conformal parameterization is important for shape analysis. For instance, the well-known conformal welding method by Sharon and Mumford [46] and the extended version by Lui et al. [34] requires a disk conformal parameterization for computing the shape fingerprints. Free-boundary parameterizations cannot be applied. The abovementioned applications demonstrate the physical significance of achieving a disk conformal parameterization.

In real applications, besides the quality of the parameterization result, it is also important to consider the computational efficiency of the parameterization algorithm. In particular, a fast algorithm is desired so that the computation can be completed within a short time. In this paper, we develop an efficient algorithm for the disk conformal parameterization of simply-connected open surfaces. To achieve the efficiency, we first transform a topologically disk-like surface to a genus-0 closed surface by a double covering technique. Then we can apply a fast parameterization algorithm for genus-0 closed surfaces to compute a spherical parameterization of the double covered surface. Note that although the size of the problem is doubled by double covering, the computational efficiency is preserved because of the symmetry of the double covered surface. The spherical parameterization, together with a suitable Möbius transformation and the stereographic projection, provides us with an almost circular planar parameterization for the original surface. A normalization technique followed by a composition of quasi-conformal maps are then used for obtaining a bijective disk conformal parameterization. The bijectivity of the parameterization is supported by quasi-conformal theories. The entire algorithm only involves solving sparse linear systems and hence the computation of the disk conformal parameterization is greatly accelerated. Specifically, our proposed method speeds up the computation of disk conformal parameterizations by over 60% while attaining accuracy comparable to the state-of-the-art approaches [4, 14]. In addition, our proposed method demonstrates robustness to highly irregular triangulations.

The rest of the paper is organized as follows. In Section 2, we review the previous works on surface parameterizations. In Section 3, we highlight the contribution of our work. Our proposed algorithm is then explained in details in Section 4. The numerical implementation of the algorithm is introduced in Section 5. In Section 6, we present numerical experiments to demonstrate the effectiveness of our proposed method. The paper is concluded in Section 7.

2 Previous works

With a large variety of real applications, surface parameterization has been extensively studied by different research groups. Readers are referred to [10, 11, 20, 49] for surveys of mesh parameterization methods. In this section, we give an overview of the works on conformal parameterization.

A practical parameterization scheme should retain the original geometric information of a surface as far as possible. Ideally, the isometric parameterization, which preserves geometric distances, is the best parameterization in the sense of geometry preserving. However, isometric planar parameterizations only exist for surfaces

with zero Gaussian curvature [6]. Hence, it is impossible to achieve isometric parameterizations for general surfaces. A similar yet far more practical substitute is the conformal parameterization. Conformal parameterizations are angle preserving, and hence the infinitesimal shape is well retained. For this reason, numerous studies have been devoted to surface conformal parameterizations.

The existing algorithms for the conformal parameterizations of disk-type surfaces can be divided into two groups, namely, the free-boundary methods and the fixed-boundary methods. For the free-boundary methods, the planar conformal parameterization results are with irregular shapes. In [18], Hormann and Greiner proposed the MIPS algorithm for conformal parameterizations of topologically disk-like surfaces. The boundary develops naturally with the algorithm. In [47], Sheffer and de Sturler proposed the Angle Based Flattening (ABF) method to compute conformal maps, based on minimizing the angular distortion in each face to the necessary and sufficient condition of a valid 2D mesh. Sheffer et al. [48] extended the ABF method to ABF++, a more efficient and robust algorithm for planar conformal parameterizations. A new numerical solution technique, a new reconstruction scheme and a hierarchical technique are used to improve the performance. Lévy et al. [25] proposed the Least-Square Conformal Maps (LSCM) to compute a conformal parameterization by approximating the Cauchy-Riemann equation using the least square method. In [5], Desbrun et al. proposed the Discrete, Natural Conformal Parameterization (DNCP) by computing the discrete Dirichlet energy. In [24], Kharevych et al. constructed a conformal parameterization based on circle patterns, which are arrangements of circles on every face with prescribed intersection angles. Jin et al. [21] applied a double covering technique [15] and an iterative scheme for genus-0 surface conformal mapping in [14] to obtain a planar conformal parameterization. In [40], Mullen et al. reported a spectral approach to discrete conformal parameterizations, which involves solving a sparse symmetric generalized eigenvalue problem.

For the fixed-boundary methods, numerous researchers have proposed brilliant disk conformal parameterization algorithms. Floater [8] proposed the shape-preserving parameterization method for surface triangulations by solving linear systems based on convex combinations. In [9], Floater improved the parameterization method using a generalization of barycentric coordinates. In [14], Gu and Yau constructed a basis of holomorphic 1-forms to compute conformal parameterizations. By integrating the holomorphic 1-forms on a mesh, a globally conformal parameterization can be obtained. In [39], Luo proposed the combinatorial Yamabe flow on the space of all piecewise flat metrics associated with a triangulated surface for the parameterization. In [22], Jin et al. suggested the discrete Ricci flow method for conformal parameterizations, based on a variational framework and circle packing. Yang et al. [50] generalized the discrete Ricci flow and improved the computation by allowing two circles to intersect or separate from each other, unlike the conventional circle packing-based method [22]. In [4], Choi and Lui presented a two-step iterative scheme to correct the conformality distortions at different regions of the unit disk. Table 1 compares several previous works on the conformal parameterizations of disk-type surfaces.

Our proposed algorithm involves a step of spherical parameterization. Various spherical parameterization algorithms have been developed in the recent few decades,

Table 1 Several previous works on conformal parameterization of simply-connected open surfaces

Methods	Boundary	Bijective?	Iterative?
Shape-preserving [8]	Fixed	Yes	No
MIPS [18]	Free	Yes	Yes
ABF/ABF++ [47, 48]	Free	Local (no flips)	Yes
LSCM/DNCP [5, 25]	Free	No	No
Holomorphic 1-form [14]	Fixed	No	No
Mean-value [9]	Fixed	Yes	No
Yamabe Riemann map [39]	Fixed	Yes	Yes
Circle patterns [24]	Free	Local (no flips)	Yes
Genus-0 surface conformal map [21]	Free	No	Yes
Discrete Ricci flow [22]	Fixed	Yes	Yes
Spectral conformal [40]	Free	No	No
Generalized Ricci flow [50]	Fixed	Yes	Yes
Two-step iteration [4]	Fixed	Yes	Yes

such as [1, 3, 13–17, 35]. Among the existing algorithms, we apply the fast spherical conformal parameterization algorithm proposed in [3], which involves solving a Laplace equation and a generalized Laplace equation. As a remark, the use of geometric PDEs is not only important in surface parameterization but also in a large variety of other fields, such as image analysis, geometric design and minimal molecular surfaces [2]. More details of the tools used in our proposed method will be explained in Section 4.

3 Contributions

In this paper, we introduce a linear formulation for the disk conformal parameterization of simply-connected open surfaces. Unlike the conventional approaches, we first find an initial map via a parameterization algorithm for genus-0 closed surfaces, with the aid of a double covering technique. The symmetry of the double covered surface helps retaining the low computational cost of the problem. After that, we normalize the boundary and apply quasi-conformal theories to ensure the bijectivity and conformality. Our proposed algorithm is advantageous in the following aspects:

1. Our proposed method only involves solving a few sparse symmetric positive definite linear systems of equations. It further accelerates the computation of disk conformal parameterizations by over 60% when compared with the fastest state-of-the-art approach [4].
2. With the significant improvement of the computational time, our proposed method possesses comparable accuracy as of the other state-of-the-art approaches.

3. The bijectivity of the parameterization is supported by quasi-conformal theories. No foldings or overlaps exist in the parameterization results.
4. Our proposed method is highly robust to irregular triangulations. It can handle meshes with very sharp and irregular triangular faces.

4 Proposed method

In this section, we present our proposed method for disk conformal parameterizations of simply-connected open surfaces in details.

A map $f : M \to N$ between two Riemann surfaces is called a *conformal map* if it preserves the inner product between vectors in parameter space and their images in the tangent plane of the surface, up to a scaling factor. More specifically, there exists a positive scalar function λ such that $f^* ds_N^2 = \lambda ds_M^2$. In other words, conformal maps are angle preserving. The following theorem guarantees the existence of several special types of conformal maps.

Theorem 4.1 (**Uniformization Theorem**) *Every simply connected Riemann surface is conformally equivalent to exactly one of the following three domains:*

(i) *the Riemann sphere,*
(ii) *the complex plane,*
(iii) *the open unit disk.*

Proof See [44]. □

With this theoretical guarantee, our goal is to efficiently and accurately compute a conformal map $f : M \to \mathbb{D}$ from a topologically disk-like surface M to the open unit disk $\mathbb{D}$.

Before explaining our proposed algorithm in details, we point out the major differences between our proposed method and the two-step iterative approach [4]. Table 2 highlights the main features of our proposed method and the two-step iterative approach [4] for disk conformal parameterizations. The two-step iterative approach makes use of the disk harmonic map as an initial map, with the arc-length parameterized circular boundary constraint. This introduces large conformality distortions in the initial map. To correct the conformality distortion, two further steps are required in [4]. First, the Cayley transform is applied to map the initial disk onto the upper half plane for correcting the distortion at the inner region of the disk. Then, iterative reflections along the unit circle are applied for correcting the distortion near the boundary of the disk until convergence.

In contrast, our proposed fast method primarily consists of only two stages. In the first stage, we find an initial planar parameterization via double covering followed by a spherical conformal map. Since there is no enforcement of the boundary in computing the initial planar parameterization, the conformality distortion of our initial map is much lower than that by the disk harmonic map. In the second stage, we enforce the circular boundary, and then alleviate the conformality distortion as well as achieving

Table 2 Features of the two-step iterative approach [4] and our proposed method

Features	Two-step iterative approach [4]	Our proposed method
Type of input surfaces	Simply-connected open surfaces	Simply-connected open surfaces
Initial map	Disk harmonic map	double covering followed by a fast spherical conformal map
Enforcement of boundary when computing the initial map	Yes	No
Method for correcting the conformality distortion	Step 1: Use the Cayley transform and work on the upper half plane Step 2: Iterative reflections along the unit circle until convergence	One-step normalization and composition of quasi-conformal maps
Output	Unit disk	Unit disk
Bijectivity	Yes	Yes
Iterations required?	Yes	No

the bijectivity using quasi-conformal theories. The absence of iterations in our proposed algorithm attributes to the significant enhancement in the computational time when compared with the two-step iterative approach [4].

In the following, we explain the two stages of our proposed algorithm in details.

4.1 Finding an initial map via double covering

Instead of directly computing the map $f : M \to \mathbb{D}$ from a simply-connected open surface M to the unit disk $\mathbb{D}$, we tackle the problem by using a simple double covering technique. The double covering technique was also suggested in [15] to compute conformal gradient field of surfaces with boundaries. In the following, we discuss the construction in the continuous setting. Specifically, we construct a genus-0 closed surface $\widetilde{M}$ by the following method. First, we duplicate M and change its orientation. Denote the new copy by M'. Then we identify the boundaries of the two surfaces:

$$\partial M \longleftrightarrow \partial M'. \tag{1}$$

By the above identification, the two surfaces M and M' are glued along the two boundaries. Note that here we do not identify the interior of the two surfaces M and M'. As a result, a closed surface is formed. Denote the new surface by $\widetilde{M}$. It can be easily noted that since M and M' are simply-connected open surfaces, the new surface $\widetilde{M}$ is a genus-0 closed surface. More explicitly, denote by K and κ_g the Gaussian curvature and geodesic curvature. Assume that we slightly edit the boundary parts of M and M' so that $\widetilde{M}$ is smooth. Then by the Gauss-Bonnet theorem, we have

$$\int_M K dA + \int_{\partial M} \kappa_g ds = 2\pi \chi(M) = 2\pi \tag{2}$$

and

$$\int_{M'} K dA + \int_{\partial M'} \kappa_g ds = 2\pi \chi(M') = 2\pi. \tag{3}$$

Hence, we have

$$\begin{aligned} 2\pi \chi(\widetilde{M}) &= \textstyle\int_{\widetilde{M}} K dA \\ &= \textstyle\int_M K dA + \int_{M'} K dA \\ &= \left(2\pi - \textstyle\int_{\partial M} \kappa_g ds\right) + \left(2\pi - \textstyle\int_{\partial M'} \kappa_g ds\right) \\ &= 4\pi - \textstyle\int_{\partial M} \kappa_g ds + \int_{\partial M} \kappa_g ds \\ &= 4\pi. \end{aligned} \tag{4}$$

Therefore, the new surface $\widetilde{M}$ has Euler characteristic $\chi(\widetilde{M}) = 2$, which implies that it is a genus-0 closed surface. As a remark, in the discrete case, the unsmooth part caused by the double covering does not cause any difficulty in our algorithm since we are only considering the angle structure of the glued mesh. The details of the combinatorial argument are explained in Section 5.

After obtaining $\widetilde{M}$ by the abovementioned double covering technique, we look for a conformal map that maps $\widetilde{M}$ to the unit sphere. By the uniformization theorem, every genus-0 closed surface is conformally equivalent to the unit sphere. Hence, the existence of such a conformal map is theoretically guaranteed. In [3], Choi et al. proposed a fast algorithm for computing a conformal map between genus-0 closed

surfaces and the unit sphere. The algorithm consists of two steps, and in each step one sparse symmetric positive definite linear system is to be solved. In the following, we briefly describe the mentioned spherical conformal parameterization algorithm.

The *harmonic energy functional* of a map $\psi : N \to \mathbb{S}^2$ from a genus-0 closed surface N to the unit sphere is defined as

$$E(\psi) = \int_N ||\nabla \psi||^2 dv_N. \tag{5}$$

In the space of mappings, the critical points of $E(\psi)$ are called *harmonic mappings*. For genus-0 closed surfaces, conformal maps are equivalent to harmonic maps [23]. Therefore, to find a spherical conformal map, we can consider solving the following Laplace equation

$$\Delta^T \psi = 0 \tag{6}$$

subject to the spherical constraint $||\psi|| = 1$, where $\Delta^T \psi$ is the tangential component of $\Delta\psi$ on the tangent plane of $\mathbb{S}^2$. Note that this problem is nonlinear. In [3], the authors linearize this problem by solving the equation on the complex plane:

$$\Delta\phi = 0 \tag{7}$$

given three point boundary correspondences $\phi(a_i) = b_i$, where $a_i, b_i \in \mathbb{C}$ for $i = 1, 2, 3$. Note that $\Delta^T \phi = \Delta\phi = 0$ since the target domain is now $\mathbb{C}$. Now the problem (7) becomes linear since $\Delta\phi$ is linear and the nonlinear constraint $||\psi|| = 1$ in the original problem (6) is removed. After solving the problem (7), the inverse stereographic projection is applied for obtaining a spherical parameterization. Note that in the discrete case, the conformality of the inner region on the complex plane is negligible but that of the outer region on the complex plane is quite large. Correspondingly, the conformality distortion near the North pole of the sphere is quite large. Therefore, to correct the conformality distortion near the North pole, the authors in [3] propose to apply the South-pole stereographic projection to project the sphere onto the complex plane. Unlike the result obtained by solving Equation (7), the part with high conformality distortion is now at the inner region on the plane. By fixing the outermost region and composing the map with a suitable quasi-conformal map, the distortion of the inner region can be corrected. Finally, by the inverse South-pole stereographic projection, a bijective spherical conformal parameterization with negligibly low distortions can be obtained. Readers are referred to [45] and [3] for more details of the harmonic map theory and the abovementioned algorithm respectively.

The combination of the double covering technique and the fast spherical conformal parameterization algorithm in [3] is particularly advantageous. It should be noted that because of the symmetry of the double covered surface, half of the entries in the coefficient matrix of the discretization of the Laplace Equation (7) are duplicated. Therefore, even we have doubled the size of the problem under the double covering technique, we can save half of the computational cost of the coefficient matrix by only computing half of the entries. Moreover, the spherical conformal parameterization algorithm in [3] involves solving only two sparse symmetric positive definite systems of equations. Therefore, the computation is still highly efficient.

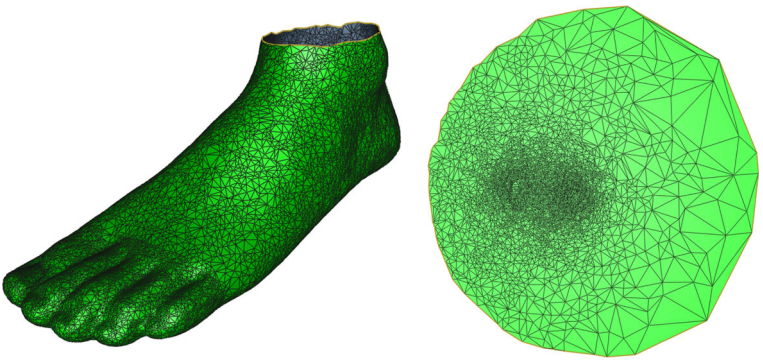

Fig. 1 A simply-connected open human foot model and the planar conformal parameterization obtained using double covering followed by spherical conformal map and stereographic projection. It can be observed that the resulting boundary is not perfectly circular

After finding a spherical conformal map $\tilde{f} : \widetilde{M} \to \mathbb{S}^2$ for the glued surface $\widetilde{M}$ using the parameterization algorithm, note that by symmetry, we can separate the unit sphere into two parts, each of which exactly corresponds to one of M and M'. Since our goal is to find a disk conformal map $f : M \to \mathbb{D}$, we put our focus on only one of the two parts. Now, we apply a Möbius transformation on $\mathbb{S}^2$ so that the two parts become the northern and southern hemispheres of $\mathbb{S}^2$. After that, by applying the stereographic projection $P : \mathbb{S}^2 \to \overline{\mathbb{C}}$ defined by

$$P(x, y, z) = \frac{x}{1-z} + i\frac{y}{1-z}, \tag{8}$$

the southern hemisphere is mapped onto the open unit disk $\mathbb{D}$. Since the Möbius transformation and the stereographic projection are both conformal mappings, the combination of the above steps provides a conformal map $f : M \to \mathbb{D}$.

Theoretically, by the symmetry of the double covered surface, the boundary of the planar region obtained by the above stereographic projection should be a perfect unit circle. However, in the discrete case, due to irregular triangulations of the meshes and the conformality distortions of the map, the boundary is usually different from a perfect circle, as suggested in the experimental results in [4]. In other words, the planar region R we obtained after applying the stereographic projection may not be a unit disk. An illustration is given in Fig. 1. To solve this issue, we need one further step to enforce the circular boundary, at the same time maintaining low conformality distortions and preserving the bijectivity of the parameterization.

4.2 Enforcing the circular boundary to achieve a bijective disk conformal parameterization

To control the conformality distortion and the bijectivity, our idea is to normalize the boundary and then compose the map with a *quasi-conformal map*. Quasi-conformal maps are a generalization of conformal maps, which are orientation preserving homeomorphisms between Riemann surfaces with bounded conformality distortions.

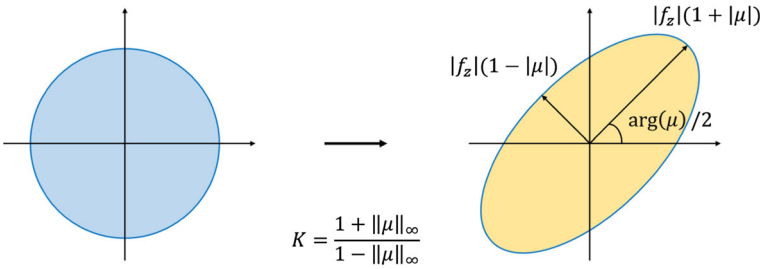

Fig. 2 An illustration of quasi-conformal mappings. All information of a quasi-conformal map can be determined by the Beltrami coefficient μ

Intuitively, a conformal mapping maps infinitesimal circles to infinitesimal circles, while a quasi-conformal mapping maps infinitesimal circles to infinitesimal ellipses with bounded eccentricity [12]. Mathematically, a *quasi-conformal map* $f : \mathbb{C} \to \mathbb{C}$ satisfies the Beltrami equation

$$\frac{\partial f}{\partial \bar{z}} = \mu(z)\frac{\partial f}{\partial z} \tag{9}$$

for some complex-valued functions μ with $\|\mu\|_\infty < 1$. μ is called the *Beltrami coefficient* of f.

The Beltrami coefficient captures the important information of the mapping f. For instance, the angles and the magnitudes of both the maximal magnification and the maximal shrinkage can be easily determined by the Beltrami coefficient μ (see Fig. 2). Specifically, the angle of the maximal magnification is $arg(\mu(p))/2$ with the magnifying factor $1 + |\mu(p)|$, and the angle of the maximal shrinkage is the orthogonal angle $(arg(\mu(p)) - \pi)/2$ with the shrinking factor $1 - |\mu(p)|$. The maximal dilation of f is given by:

$$K(f) = \frac{1 + \|\mu\|_\infty}{1 - \|\mu\|_\infty}. \tag{10}$$

It is also noteworthy that f is conformal around a small neighborhood of p if and only if $\mu(p) = 0$. Hence, $|\mu|$ is a good indicator of the angular distortions of a mapping.

In fact, the norm of the Beltrami coefficient μ is not only related to the conformality distortion but also the bijectivity of the associated quasi-conformal mapping, as explained by the following theorem:

Theorem 4.2 *If $f : M \to \mathbb{D}$ is a C^1 map satisfying $\|\mu_f\|_\infty < 1$, then f is bijective.*

Proof See [12]. □

This theorem can be explained with the aid of the Jacobian of f. The Jacobian J_f of f is given by

$$J_f = \left|\frac{\partial f}{\partial z}\right|^2 (1 - |\mu_f|^2). \tag{11}$$

Suppose $\|\mu_f\|_\infty < 1$, then we have $\left|\frac{\partial f}{\partial z}\right|^2 \neq 0$ and $(1 - |\mu_f|^2) > 0$. Therefore, $J(f)$ is positive everywhere. Since $\mathbb{D}$ is simply-connected and f is proper, we can conclude that f is a diffeomorphism. In fact, f is a universal covering map of degree 1. Therefore, f must be bijective. One important consequence of Theorem 4.2 is that we can easily achieve the bijectivity of a quasi-conformal map by enforcing its associated Beltrami coefficient to be with supremum norm less than 1.

Moreover, it is possible for us to reconstruct a mapping by a given Beltrami coefficient, as explained by the following theorem:

Theorem 4.3 *Let M_1 and M_2 be two simply-connected open surfaces. Given 2-point correspondences, every Beltrami coefficient μ with $\|\mu\| < 1$ is associated with a unique quasi-conformal homeomorphism $f : M_1 \to M_2$.*

Proof See [12]. □

For the aspect of numerical computations, Lui et al. [33] proposed the linear Beltrami solver (**LBS**), a fast algorithm for reconstructing a quasi-conformal map on a rectangular domain from a given Beltrami coefficient. The key idea of **LBS** is as follows.

By expanding the Beltrami Equation (9), we have

$$\mu_f = \frac{(u_x - v_y) + i(v_x + u_y)}{(u_x + v_y) + i(v_x - u_y)}. \tag{12}$$

Suppose $\mu(f) = \rho + i\tau$. Then, v_x and v_y can be expressed as linear combinations of u_x and u_y:

$$\begin{aligned} v_y &= \alpha_1 u_x + \alpha_2 u_y, \\ -v_x &= \alpha_2 u_x + \alpha_3 u_y, \end{aligned} \tag{13}$$

where

$$\begin{aligned} \alpha_1 &= \tfrac{(\rho-1)^2+\eta^2}{1-\rho^2-\eta^2}, \\ \alpha_2 &= -\tfrac{2\eta}{1-\rho^2-\eta^2}, \\ \alpha_3 &= \tfrac{1+2\rho+\rho^2+\eta^2}{1-\rho^2-\eta^2}. \end{aligned} \tag{14}$$

Similarly, we can express u_x and u_y as linear combinations of v_x and v_y:

$$\begin{aligned} -u_y &= \alpha_1 v_x + \alpha_2 v_y, \\ u_x &= \alpha_2 v_x + \alpha_3 v_y. \end{aligned} \tag{15}$$

Hence, to solve for a quasi-conformal map, it remains to solve

$$\nabla \cdot \left(A \begin{pmatrix} u_x \\ u_y \end{pmatrix} \right) = 0 \text{ and } \nabla \cdot \left(A \begin{pmatrix} v_x \\ v_y \end{pmatrix} \right) = 0 \tag{16}$$

where $A = \begin{pmatrix} \alpha_1 & \alpha_2 \\ \alpha_2 & \alpha_3 \end{pmatrix}$.

In the discrete case, the above elliptic PDEs (16) can be discretized into sparse linear systems. For details, please refer to [33]. In the following discussion, we denote

the quasi-conformal map associated with the Beltrami coefficient μ obtained by **LBS** by **LBS**(μ).

Another important property of quasi-conformal mappings is about their composition mappings. In fact, the Beltrami coefficient of a composition mapping can be explicitly expressed in terms of the Beltrami coefficients of the original mappings.

Theorem 4.4 *Let $f : \Omega \subset \mathbb{C} \to f(\Omega)$ and $g : f(\Omega) \to \mathbb{C}$ be two quasi-conformal mappings. Then the Beltrami coefficient of $g \circ f$ is given by*

$$\mu_{g\circ f} = \frac{\mu_f + (\overline{f_z}/f_z)(\mu_g \circ f)}{1 + (\overline{f_z}/f_z)\overline{\mu_f}(\mu_g \circ f)}. \tag{17}$$

In particular, if $\mu_{f^{-1}} \equiv \mu_g$, then since $\mu_{f^{-1}} \circ f = -(f_z/\overline{f_z})\mu_f$, we have

$$\mu_{g\circ f} \equiv \frac{\mu_f + (\overline{f_z}/f_z)((-f_z/\overline{f_z})\mu_f)}{1 + (\overline{f_z}/f_z)\overline{\mu_f}((-f_z/\overline{f_z})\mu_f)} \equiv 0. \tag{18}$$

Hence $g \circ f$ is conformal.

Proof See [12]. □

In other words, by composing two quasi-conformal maps whose Beltrami coefficients satisfy the above condition, one can immediately obtain a conformal map. This observation motivates the following step.

To enforce the circular boundary of the parameterization, we first normalize the boundary of the region R to the unit circle:

$$v \mapsto \frac{v}{|v|} \tag{19}$$

for all $v \in \partial R$. Denote the normalized region by $\widetilde{R}$. Since the vertices near the boundary of the region R may be very dense, a direct normalization of the boundary may cause overlaps of the triangulations as well as geometric distortions on the unit disk. To eliminate the overlaps and the distortions of $\widetilde{R}$, we apply the linear Beltrami solver to construct another quasi-conformal map with the normalized boundary constraints. Then by the composition property, the composition map becomes a conformal map. More specifically, denote the Beltrami coefficient of the mapping $g : \widetilde{R} \to M$ from the normalized planar region to the original surface by μ. We reconstruct a quasi-conformal map with Beltrami coefficient μ on the unit disk by extending the linear Beltrami solver, so that it is applicable not only on rectangular domains but also circular domains. We compute a map $h : \widetilde{R} \to \mathbb{D}$ by applying the linear Beltrami solver:

$$h = \mathbf{LBS}(\mu) \tag{20}$$

with the circular boundary constraint $h(v) = v$ for all$v \in \partial\widetilde{R}$.

Note that by the composition property stated in Theorem 4.4, $h \circ g^{-1}$ is a conformal map from the original surface M to the unit disk $\mathbb{D}$. Finally, the bijectivity of the composition map is supported by Theorem 4.2, since the Beltrami coefficient of the

composition map is with supremum norm less than 1. This completes the task of finding a bijective disk conformal parameterization. The numerical implementation of our proposed method is explained in Section 5.

5 Numerical implementation

In this section, we describe the numerical implementation of our proposed algorithm in details. In the discrete case, 3D surfaces are commonly represented by triangular meshes. Discrete analogs of the theories on the smooth surfaces are developed on the triangulations.

We first briefly describe the discrete version of the mentioned double covering technique for obtaining a genus-0 closed mesh. This discretization was also applied in [15] to compute conformal gradient fields of surfaces with boundaries. A triangulation $K = (V, E, F)$ of a smooth simply-connected open surface consists of the vertex set V, the edge set E and the triangular face set F. Each face can be represented as an ordered triple $[u, v, w]$ where u, v, w are three vertices. Suppose the boundary vertices of K are $\{w_i\}_{i=1}^r$. Denote a duplicated triangulation of K by $K' = (V', E', F')$, with boundary vertices $\{w_i'\}_{i=1}^r$. Let v, e, f denote the number of vertices, edges and faces of M respectively. We duplicate M and denote the new copy by M', with v', e', f' the number of vertices, edges and faces. By Euler's formula, we have

$$v - e + f = v' - e' + f' = 1. \tag{21}$$

Then, we construct a new surface $\widetilde{M}$ by reversing the face orientation of M' and gluing the two boundaries ∂M and $\partial M'$. To reverse the orientation of K', we rearrange the order of the vertices of each face in F' from $[u, v, w]$ to $[u, w, v]$. Then, to glue the two surfaces, we identify the boundary vertices of the two meshes:

$$w_i \longleftrightarrow w_i' \text{ for all} i = 1, 2, \cdots, r. \tag{22}$$

Now, denote the number of vertices, edges and faces of $\widetilde{M}$ by $\tilde{v}, \tilde{e}$ and $\tilde{f}$ respectively. It follows that

$$\begin{aligned} &\tilde{v} - \tilde{e} + \tilde{f} \\ &= (v + v' - r) - (e + e' - r) + (f + f') \\ &= v + v' - e - e' + f + f' \\ &= 2, \end{aligned} \tag{23}$$

Hence, the new surface $\widetilde{M}$ is a genus-0 closed surface. The complete double covering procedure is described in Algorithm 1.

Then, we introduce the discretization about harmonic mappings used in the fast spherical conformal parameterization algorithm in [3]. Let $\widetilde{K}$ be the triangulation of a genus-0 closed surface N. Let us denote the edge spanned by two vertices u, v on $\widetilde{K}$ by $[u, v]$. The *discrete harmonic energy* of $\psi : \widetilde{K} \to \mathbb{S}^2$ is given by

$$E(\psi) = \frac{1}{2} \sum_{[u,v] \in \widetilde{K}} k_{uv} ||\psi(u) - \psi(v)||^2, \tag{24}$$

Algorithm 1: The double covering technique in our initial step.

Input: A triangulation $K = (V, E, F)$ of a simply-connected open surface.
Output: A genus-0 closed mesh $\widetilde{K} = (\widetilde{V}, \widetilde{E}, \widetilde{F})$.

1 Duplicate K and denote the copy by $K' = (V', E', F')$;
2 Change the order of the vertices of each face in F' from $[u, v, w]$ to $[u, w, v]$;
3 Replace the boundary vertices w_i' by w_i in E' and F' for $i = 1, 2, \cdots, r$;
4 Set $\widetilde{V} = V \cup V' \setminus \{w_i'\}_{i=1}^{r}$;
5 Set $\widetilde{E} = E \cup E'$;
6 Set $\widetilde{F} = E \cup E'$;

where $k_{uv} = \cot\alpha + \cot\beta$ with α, β being the angles opposite to the edge $[u, v]$. This is known as the cotangent formula [41]. With the discrete harmonic energy, we can appropriately discretize the Laplace-Beltrami operator as

$$\Delta\psi(v_i) = \sum_{v_j \in N(v_i)} k_{v_i v_j}(\psi(v_j) - \psi(v_i)), \tag{25}$$

where $N(v_i)$ denotes the set of the 1-ring neighboring vertices of v_i. Therefore, the Laplace Equation (7) becomes a linear system in the form

$$Az = b, \tag{26}$$

where A is a square matrix satisfying

$$A_{ij} = \begin{cases} k_{v_i v_j} & \text{if} i \neq j, \\ -\sum_{v_t \in N(v_i)} k_{v_i v_t} & \text{if} i = j \end{cases} \quad \text{for all} i, j. \tag{27}$$

For the choice of the points $a_1, a_2, a_3, b_1, b_2, b_3$ in the boundary constraint of Equation (7), we choose a triangular face $[a_1, a_2, a_3]$ on the triangulation K and a triangle $[b_1, b_2, b_3]$ on the complex plane that shares the same angle structure as $[a_1, a_2, a_3]$. Note that the above linear system is sparse and symmetric positive definite. Therefore, it can be efficiently solved.

It is noteworthy that due to the symmetry of the double covered surface, for every edge $[u, v]$ in the triangulation K, there exists a unique edge $[u', v']$ in the duplicated triangulation K' such that

$$k_{uv} = \cot\alpha + \cot\beta = \cot\alpha' + \cot\beta' = k_{u'v'}, \tag{28}$$

where α, β are the angles opposite to the edge $[u, v]$ and α', β' are the angles opposite to the edge $[u', v']$. Therefore, only half of the vertices and faces are needed for

computing the whole coefficient matrix A to solve the Laplace Equation (7). More explicitly, Equation (26) can be expressed as the following form:

$$\begin{pmatrix} B & * & 0 \\ * & * & * \\ 0 & * & B \end{pmatrix} \begin{pmatrix} z_1 \\ \vdots \\ z_{|V|-r} \\ \zeta_1 \\ \vdots \\ \zeta_r \\ z'_1 \\ \vdots \\ z'_{|V|-r} \end{pmatrix} = b. \tag{29}$$

Here, $\{z_i\}_{i=1}^{|V|-r}$ and $\{z'_i\}_{i=1}^{|V|-r}$ are respectively the coordinates of the non-boundary vertices of K and K', $\{\zeta_i\}_{i=1}^{r}$ are the coordinates of the glued vertices, and B is a $(|V|-r) \times (|V|-r)$ sparse symmetric positive definite matrix. It follows that we can save half of the computational cost in finding all the cotangent weights k_{uv} in A. Hence, the computation of the spherical conformal map is efficient even the number of vertices and faces is doubled under the double covering step.

Another important mathematical tool in our proposed algorithm is the quasi-conformal mapping. Quasi-conformal mappings are closely related to the Beltrami coefficients. It is important to establish algorithms for computing the Beltrami coefficient associated with a given quasi-conformal map, as well as for computing the quasi-conformal map associated with a given Beltrami coefficient.

We first focus on the computation of the Beltrami coefficients. In the discrete case, suppose $K_1, K_2 \subset \mathbb{R}^3$ are two triangular meshes with the same number of vertices, faces and edges, and $f : K_1 \to K_2$ is an orientation preserving piecewise linear homeomorphism. It is common to discretize the Beltrami coefficient on the triangular faces. To compute the Beltrami coefficient μ_f associated with f, we compute the partial derivatives on every face T_1 on K_1.

Suppose T_1 on K_1 corresponds to a triangular face T_2 on K_2 under the mapping f. The approximation of μ_f on T_1 can be computed using the coordinates of the six vertices of T_1 and T_2. Since the triangulations are piecewise linear, we can place T_1 and T_2 on $\mathbb{R}^2$ using suitable rotations and translations to simplify the computations. Hence, without loss of generality, we can assume that T_1 and T_2 are on $\mathbb{R}^2$. Specifically, suppose $T_1 = [a_1 + i\, b_1, a_2 + i\, b_2, a_3 + i\, b_3]$ and $T_2 = [w_1, w_2, w_3]$, where $a_1, a_2, a_3, b_1, b_2, b_3 \in \mathbb{R}$, and $w_1, w_2, w_3 \in \mathbb{C}$. Recall that $\frac{\partial f}{\partial \bar{z}} = \frac{1}{2}\left(\frac{\partial f}{\partial x} + i\frac{\partial f}{\partial y}\right)$ and $\frac{\partial f}{\partial z} = \frac{1}{2}\left(\frac{\partial f}{\partial x} - i\frac{\partial f}{\partial y}\right)$. Hence, to discretize the Beltrami coefficient, we only need to compute $\frac{\partial}{\partial x}$ and $\frac{\partial}{\partial y}$ on every triangular face T_1. It is natural to use the differences between the vertex coordinates for the approximation. We define

$$D_x = \frac{1}{2Area(T_1)} \begin{pmatrix} b_3 - b_2 \\ b_1 - b_3 \\ b_2 - b_1 \end{pmatrix}^t \quad \text{and} \quad D_y = -\frac{1}{2Area(T_1)} \begin{pmatrix} a_3 - a_2 \\ a_1 - a_3 \\ a_2 - a_1 \end{pmatrix}^t. \tag{30}$$

Then, we can compute the Beltrami coefficient

$$\mu_f(z) = \frac{\partial f}{\partial \bar{z}} \Big/ \frac{\partial f}{\partial z} \tag{31}$$

on T_1 by

$$\mu_f(T_1) = \frac{\frac{1}{2}\left(D_x + i\ D_y\right)\begin{pmatrix} w_1 \\ w_2 \\ w_3 \end{pmatrix}}{\frac{1}{2}\left(D_x - i\ D_y\right)\begin{pmatrix} w_1 \\ w_2 \\ w_3 \end{pmatrix}}. \tag{32}$$

This approximation is easy to compute. Hence, it is convenient to obtain the Beltrami coefficient associated with a given quasi-conformal map in the discrete case. A relatively complicated task is to compute the quasi-conformal map f associated with a given Beltrami coefficient μ_f. To achieve this, we apply the **LBS** [33] to reconstruct a quasi-conformal map from a given Beltrami coefficient, with the boundary vertices of the disk fixed. We now briefly explain the discretization of the **LBS**.

Recall that the quasi-conformal map associated with a given Beltrami coefficient can be obtained by solving Equation (16). The key idea of **LBS** is to discretize Equation (16) into sparse SPD linear systems of equations so that the solution can be efficiently computed.

For each vertex v_i, let N_i be the collection of the neighboring faces attached to v_i. Let $T = [v_i, v_j, v_k]$ be a face ,$w_i = f(v_i)$, $w_j = f(v_j)$ and $w_k = f(v_k)$. Suppose $v_l = g_l + i\ h_l$ and $w_l = s_l + i\ t_l$, for $l = i, j, k$. We further denote the Beltrami coefficient of the face T obtained from Equation (32) by $\mu_f(T) = \rho_T + i\ \eta_T$. Equation (14) can be discretized as follows:

$$\begin{aligned} \alpha_1(T) &= \tfrac{(\rho_T-1)^2+\eta_T^2}{1-\rho_T^2-\eta_T^2}, \\ \alpha_2(T) &= -\tfrac{2\eta_T}{1-\rho_T^2-\eta_T^2}, \\ \alpha_3(T) &= \tfrac{1+2\rho_T+\rho_T^2+\eta_T^2}{1-\rho_T^2-\eta_T^2}. \end{aligned} \tag{33}$$

Then, Lui et al. [33] introduced the discrete divergence to compute the divergence operator. Define A_i^T, A_j^T, A_k^T, B_i^T, B_j^T, B_k^T by

$$\begin{pmatrix} A_i^T \\ A_j^T \\ A_k^T \end{pmatrix} = \frac{1}{Area(T)} \begin{pmatrix} h_j - h_k \\ h_k - h_i \\ h_i - h_j \end{pmatrix} \text{ and } \begin{pmatrix} B_i^T \\ B_j^T \\ B_k^T \end{pmatrix} = \frac{1}{Area(T)} \begin{pmatrix} g_k - g_j \\ g_i - g_k \\ g_j - g_i \end{pmatrix}. \tag{34}$$

Then the discrete divergence of a discrete vector field $\vec{V} = (V_1, V_2)$ on the triangular faces can be defined by

$$Div(\vec{V})(v_i) = \sum_{T \in N_i} A_i^T V_1(T) + B_i^T V_2(T). \tag{35}$$

With the discrete divergence, Equation (16) can be discretized into the following linear system:

$$\begin{aligned} \textstyle\sum_{T\in N_i} A_i^T[\alpha_1(T)a_T + \alpha_2(T)b_T] + B_i^T[\alpha_2(T)a_T + \alpha_3(T)b_T] = 0 \\ \textstyle\sum_{T\in N_i} A_i^T[\alpha_1(T)c_T + \alpha_2(T)d_T] + B_i^T[\alpha_2(T)c_T + \alpha_3(T)d_T] = 0 \end{aligned} \tag{36}$$

for all vertices v_i. Here a_T, b_T, c_T and d_T are certain linear combinations of the x-coordinates and y-coordinates of the desired quasi-conformal map f. Hence, we can obtain the x-coordinate and y-coordinate function of f by solving the linear system in Equation (36). For more details, please refer to [33].

With the aforementioned discrete analogs and algorithms, we are ready to describe the numerical implementation of our proposed algorithm for disk conformal parameterizations of simply-connected open surfaces.

Given a triangular mesh M of disk topology, we first apply the double covering technique as described in Algorithm 1. Then, we apply the fast spherical conformal parameterization algorithm [3] on the glued genus-0 closed mesh $\widetilde{M}$. To obtain a planar parameterization from the obtained parameter sphere S, we apply a Möbius transformation to locate the part corresponding to one of the two copies on the southern hemisphere. After that, by the stereographic projection, the Southern hemisphere is mapped to a planar region R in the complex plane. Note that this planar region is usually a bit different from a perfect disk due to the discretization and approximation errors. Therefore, we normalize the boundary of R to enforce a circular boundary as in Equation (19). However, this step may causes overlaps as well as conformality distortions on the normalized region R.

To overcome these issues, we apply the idea of the composition of quasi-conformal maps in Theorem 4.4. We first compute the Beltrami coefficient of the quasi-conformal map $g : \widetilde{R} \to M$ by solving Equation (32) on all triangular faces of $\widetilde{R}$. Denote the Beltrami coefficient by μ. We then reconstruct another quasi-conformal map $h : \widetilde{R} \to \mathbb{D}$ with the given Beltrami coefficient μ, using **LBS** [33]. Note that boundary constraints are needed in solving Equation (36). In our case, we give the Dirichlet condition on the whole boundary of the normalized disk $\widetilde{R}$. More explicitly, the boundary condition used in solving Equation (36) for the map $h : \widetilde{R} \to \mathbb{D}$ is

$$h(v) = v \tag{37}$$

for all boundary vertices $v \in \partial\widetilde{R}$. After obtaining h, we can conclude that the composition map $f = h \circ g^{-1}$ is the desired disk conformal parameterization. The complete implementation of our algorithm is described in Algorithm 2.

6 Experimental results

In this section, we demonstrate the effectiveness of our proposed algorithm using a number of 3D simply-connected open meshes. The meshes are freely adapted from mesh repositories such as the AIM@SHAPE Shape Repository [52], the Stanford 3D Scanning Repository [53] and the Benchmark for 3D Mesh Segmentation [54]. Our proposed algorithm and the two-step iterative approach [4] are implemented in MATLAB. The sparse linear systems in our proposed algorithm are solved using the

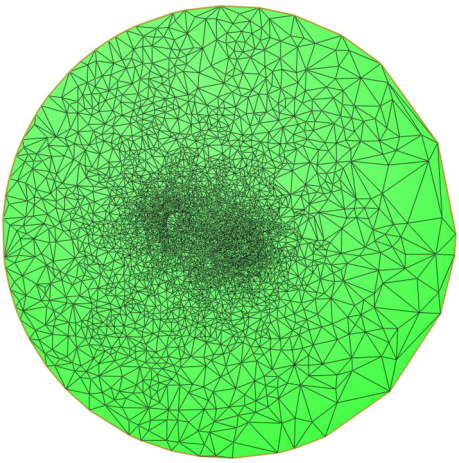

Fig. 3 The disk conformal parameterization of the foot model in Figure 1 using our proposed algorithm

backslash operator (\) in MATLAB. For the other existing algorithms in our comparison, we use available online software for the computation. All experiments are performed on a PC with a 3.40 GHz quad core CPU and 16 GB RAM.

We apply our proposed algorithm on various kinds of simply-connected open surfaces with different geometry. Figure 3 shows the disk conformal parameterization of the foot model in Fig. 1 using our proposed method. Figures 4 and 5 respectively show a simply-connected open statue model and a Stanford bunny model, together with the disk conformal parameterizations of them obtained by our proposed method. For a better visualization of the parameterization results, the triangular faces of the meshes are colored with the mean curvatures of the models. The disk parameterizations well resemble the original models locally. The histograms of the conformality distortion of our proposed algorithm are shown in Fig. 6. It can be observed that both the angle differences and the norm of the Beltrami coefficients highly concentrate at 0. This indicates that our proposed algorithm produces disk conformal parameterizations with minimal distortions for different kinds of simply-connected open surfaces.

Fig. 4 A simply-connected open statue model and the disk conformal parameterization obtained by our proposed algorithm. The color represents the mean curvature of the model

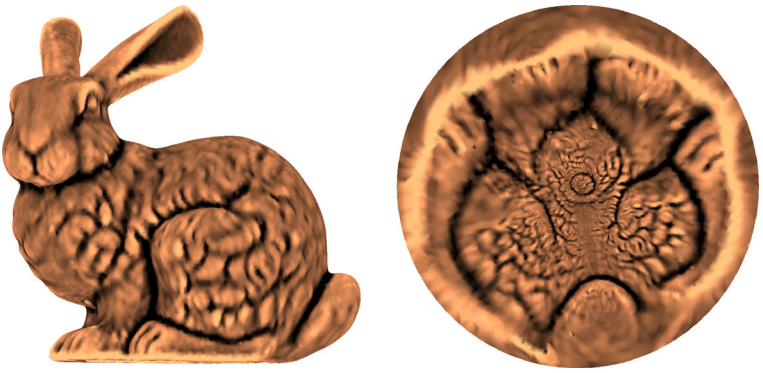

Fig. 5 A simply-connected open Stanford bunny model and the disk conformal parameterization obtained by our proposed algorithm. The color represents the mean curvature of the model

As for the efficiency, our proposed algorithm takes only around 1 second for moderate meshes. The computation can also be complete within half a minute for dense meshes.

To quantitatively assess the performance of our proposed algorithm for disk conformal parameterizations, we compare our proposed algorithm with the existing

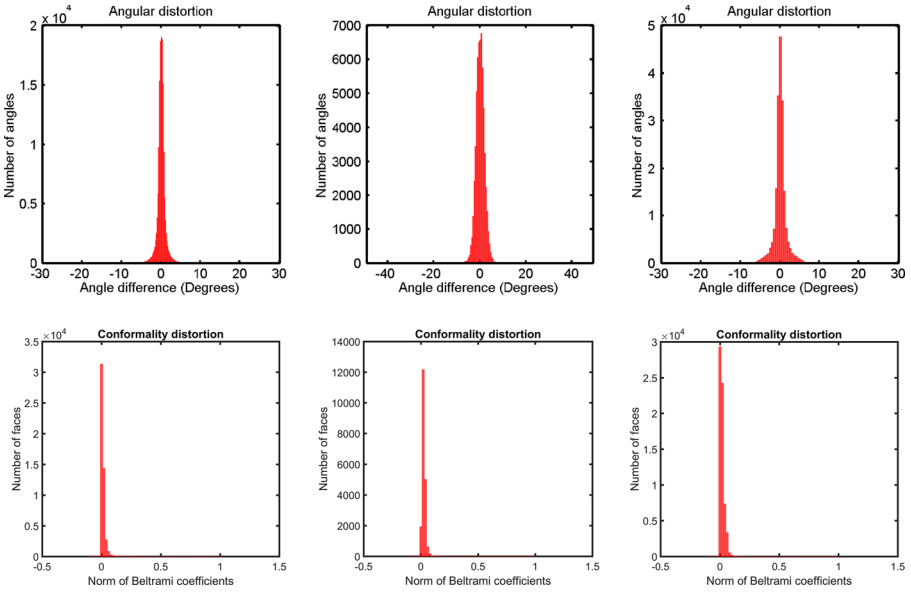

Fig. 6 The conformality distortion of our parameterization algorithm evaluated by two measurements. The *top row* shows the angular distortion of the parameterizations, in terms of the difference in degrees between the new angle after the parameterization and its corresponding original angle on the mesh. The *bottom row* shows the norm of the Beltrami coefficients of the parameterizations. The *left column*: The results of statue. The *middle column*: The results of foot. The *right column*: The results of Stanford bunny

Algorithm 2: Our proposed linear formulation for disk conformal parameterization

Input: A simply-connected open mesh M.
Output: A bijective disk conformal parameterization $f : M \to \mathbb{D}$.

1 Double cover M and obtain a genus-0 closed mesh $\widetilde{M}$;
2 Apply the fast spherical conformal parameterization [3] on $\widetilde{M}$ and obtain the parameter sphere S;
3 Apply a Möbius transformation on S so that the original surface M corresponds to the southern hemisphere of S;
4 Using the stereographic projection for the southern hemisphere of S, obtain a planar region R;
5 Normaliz the boundary of R:

$$v \mapsto \frac{v}{|v|} \tag{38}$$

for all $v \in \partial R$ and denote the normalized region by $\widetilde{R}$;
6 Compute the Beltrami coefficient of the map $g : \widetilde{R} \to M$ and denote it by μ;
7 Apply the linear Beltrami solver [33] to obtain a map $h : \widetilde{R} \to \mathbb{D}$

$$h = \mathbf{LBS}(\mu) \tag{39}$$

with the boundary constraint $h(v) = v$ for all $v \in \partial\widetilde{R}$. The composition map $f = h \circ g^{-1}$ is the desired disk conformal parameterization;

methods. In particular, the comparisons performed in [4] suggest that the holomorphic 1-form method [14] and the two-step iterative approach [4] achieve the best conformality among all state-of-the-art approaches as well as the bijectivity. Therefore, the holomorphic 1-form method and the two-step iterative approach are considered in our comparisons. The implementation of the holomorphic 1-form method is included in the RiemannMapper Toolkit [55] written in C++ and the two-step iterative approach is implemented in MATLAB. The error thresholds in both the holomorphic 1-form method and the two-step iterative approach are set to be $\epsilon = 10^{-5}$.

The statistics of the performances of the algorithms are shown in Table 3. It is noteworthy that the angular distortion of our proposed method is comparable and sometimes better than the two state-of-the-art algorithms [4, 14]. This implies that our algorithm successfully produces low-distortion parameterizations. Moreover, our proposed method demonstrates a significant improvement in the computational time of the disk conformal parameterizations. Specifically, our proposed method is around 20 times faster than the holomorphic 1-form method on average. Also, our proposed method requires 60% less computational time than the two-step iteration on average. The results illustrate the efficiency of our proposed algorithm. As a remark, in all experiments, our proposed algorithm generates folding-free parameterization results.

Table 3 Performance of our proposed method and two other state-of-the-art algorithms

		Time (s) / Mean($\|distortion\|$) (degrees) / SD($\|distortion\|$) (degrees)		
Surfaces	No. of faces	Holomorphic 1-form [14]	Two-step iteration [4]	Our proposed method
Horse	9K	fail	0.76 / 4.58 / 5.45	0.18 / 4.60 / 5.49
T-shirt	14K	18.64 / 1.38 / 3.26	2.09 / 1.34 / 3.25	0.34 / 1.35 / 3.26
Foot	20K	11.73 / 1.40 / 1.24	1.75 / 1.42 / 1.22	0.47 / 1.42 / 1.22
Chinese lion	30K	29.87 / 1.44 / 2.05	2.70 / 1.42 / 2.04	0.92 / 1.42 / 2.05
Sophie	40K	28.29 / 0.36 / 0.61	5.87 / 0.34 / 0.60	1.31 / 0.35 / 0.60
Bimba	50K	28.04 / 1.29 / 1.78	2.22 / 1.22 / 1.74	1.32 / 1.22 / 1.75
Human face	50K	28.45 / 0.55 / 1.84	4.61 / 0.53 / 1.82	1.40 / 0.53 / 1.83
Niccolo da Uzzano	50K	29.49 / 0.78 / 1.73	7.95 / 0.75 / 1.75	1.34 / 0.76 / 1.74
Mask	60K	fail	7.08 / 0.25 / 0.33	1.93 / 0.25 / 0.33
Bunny	70K	40.14 / 1.08 / 1.80	4.18 / 1.08 / 1.79	1.99 / 1.08 / 1.79
Brain	100K	58.49 / 1.46 / 1.59	6.81 / 1.46 / 1.59	2.73 / 1.46 / 1.59
Lion vase	100K	93.64 / 1.44 / 1.91	5.34 / 1.27 / 1.75	2.64 / 1.27 / 1.76
Max Planck	100K	75.92 / 0.61 / 0.80	6.58 / 0.61 / 0.80	2.88 / 0.61 / 0.80
Hand	110K	63.90 / 1.40 / 1.99	7.51 / 1.21 / 1.31	3.30 / 1.21 / 1.31
Igea	270K	173.60 / 0.40 / 0.72	54.63 / 0.40 / 0.71	9.47 / 0.40 / 0.71
Julius Caesar	430K	295.63 / 0.21 / 0.67	65.54 / 0.20 / 0.67	19.51 / 0.20 / 0.67

Here the distortion refers to the angular distortion of the parameterization, that is, the difference (in degrees) between the new angle and its corresponding original angle on the mesh

Our proposed method is very robust to irregular triangulations. Figure 7 shows a simply-connected mask model which has a very irregular triangulation. Sharp and irregular triangles can be easily observed in a zoom-in of the model. Note that the

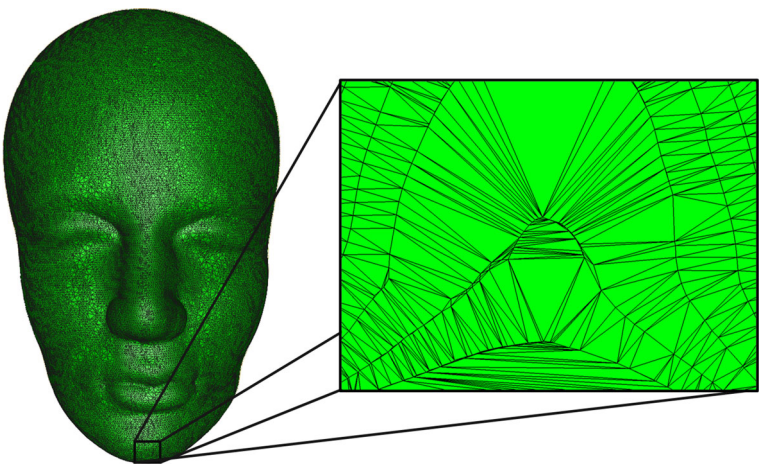

Fig. 7 A mask model with a highly irregular triangulation. *Sharp triangles* can be easily observed in a zoom-in of the model. Our proposed method can handle this kind of irregular triangulations. *Left*: The mask model. *Right*: A zoom-in of the model

Fig. 8 The Stanford bunny model with a rainbow checkerboard texture mapped onto it using our proposed parameterization algorithm

holomorphic 1-form method [14] fails to compute the disk conformal parameterization of this model while our proposed method succeeds (please refer to Table 3). This demonstrates the robustness of our proposed method.

In addition, to illustrate the accuracy of our proposed algorithm, we map a rainbow checkerboard texture onto a simply-connected bunny mesh using our proposed parameterization algorithm. In Fig. 8, it can be easily observed that the orthogonal checkerboard structure is well preserved under the our proposed parameterization scheme. The preservation of the orthogonality indicates that our proposed algorithm is with negligibly low conformality distortion.

Because of the efficiency, accuracy, bijectivity and robustness, our proposed algorithm is highly practical in applications, such as texture mapping in computer

Fig. 9 A T-shirt model with a flower pattern design mapped onto it using our proposed parameterization algorithm

graphics and fashion design. For instance, clothing designs can be easily visualized using our proposed algorithm. Figure 9 shows a T-shirt model with a 2D flower pattern design mapped onto it. It is noteworthy that the patterns are well preserved on the 3D T-shirt model. Unlike the traditional 2D images of clothes, the 3D models with our texture mapping technique provide a more comprehensive and realistic preview of the clothes for the designers. In addition, our proposed algorithm can be used in developing virtual dressing rooms. In virtual dressing rooms, it is desirable to have an efficient and accurate way for customers to virtually try on clothes. Our proposed algorithm can help creating such a virtual dressing experience for online shoppers.

As a final remark, we discuss the possibility of further boosting up the efficiency of our proposed algorithm. Recall that in our proposed algorithm, we need to compute the spherical conformal parameterization of the double covered surface using the algorithm in [3] in order to find an initial planar parameterization. The algorithm in [3] consists of two major steps, namely a North-pole step and a South-pole step. In the North-pole step, the Laplace equation (7) is solved in a triangular domain $[b_1, b_2, b_3]$ on the complex plane and the inverse stereographic projection is applied. Then the South-pole step aims to correct the conformality distortion near the North pole of the sphere caused by the discretization and approximation errors. In fact, since we are only interested in half of the glued surface, the South-pole step may be skipped as we can take the Southern hemisphere obtained by the first step as our result. It may already be with acceptable conformality.

The conformality distortion in the North-pole step in [3] is primarily caused by the choice of the boundary triangle $[a_1, a_2, a_3]$. If the chosen boundary triangle and its neighboring triangular faces are regular enough, then the overall distortion obtained in the North-pole step is already very low and only a small region around the North-pole is with relatively large distortion. In this case, the South-pole step is not needed to improve the distortion of the Southern region which we are interested. On the other hand, with the presence of the South-pole step, the overall distortion in the final spherical parameterization result will be negligible regardless of the choice of the boundary triangle. In short, with a well chosen boundary triangle $[a_1, a_2, a_3]$ in Equation (7), half of the computational cost in computing the spherical conformal mapping can be further reduced.

Table 4 shows the performance of the current version of our proposed method and the possible improved version of it without the South-pole step in [3], under a suitable choice of the boundary triangle $[a_1, a_2, a_3]$ in Equation (7). It can be noted that the differences in the conformality distortion of the two versions are mostly negligible, while the version without the South-pole step possess a further 40% improvement in the computational time on average. However, it should be reminded that the possible improved version without the South-pole step requires a suitably chosen boundary triangle $[a_1, a_2, a_3]$ for [3], while the current version of our method is fully automatic. Hence, the current version of our proposed method is probably more suitable for practical applications until an automatic algorithm for searching for the most suitable boundary triangle $[a_1, a_2, a_3]$ is developed.

Table 4 Performance of the current version of our proposed method and a possible improved version of it without the South-pole step in [3], provided a suitable choice of the boundary triangle in Equation (7)

		Time (s) / Mean($\|distortion\|$) (degrees) / SD($\|distortion\|$) (degrees)	
Surfaces	No. of faces	Our proposed method	Our proposed method without the South-pole step in [3]
Horse	9K	0.18 / 4.60 / 5.49	0.11 / 4.63 / 5.50
T-shirt	14K	0.34 / 1.35 / 3.26	0.22 / 1.37 / 3.27
Foot	20K	0.47 / 1.42 / 1.22	0.31 / 1.43 / 1.23
Chinese lion	30K	0.92 / 1.42 / 2.05	0.56 / 1.43 / 2.05
Sophie	40K	1.31 / 0.35 / 0.60	0.81 / 0.37 / 0.62
Bimba	50K	1.32 / 1.22 / 1.75	0.75 / 1.23 / 1.76
Human face	50K	1.40 / 0.53 / 1.83	0.83 / 0.55 / 1.84
Niccolo da Uzzano	50K	1.34 / 0.76 / 1.74	0.78 / 0.77 / 1.74
Mask	60K	1.93 / 0.25 / 0.33	1.22 / 0.28 / 0.37
Bunny	70K	1.99 / 1.08 / 1.79	1.14 / 1.09 / 1.79
Brain	100K	2.73 / 1.46 / 1.59	1.55 / 1.49 / 1.60
Lion vase	100K	2.64 / 1.27 / 1.76	1.45 / 1.28 / 1.76
Max Planck	100K	2.88 / 0.61 / 0.80	1.54 / 0.63 / 0.80
Hand	110K	3.30 / 1.21 / 1.31	1.74 / 1.22 / 1.31
Igea	270K	9.47 / 0.40 / 0.71	5.22 / 0.54 / 0.74
Julius Caesar	430K	19.51 / 0.20 / 0.67	12.41 / 0.21 / 0.68

7 Conclusion and future works

In this paper, we have proposed a linear formulation for the disk conformal parameterizations of simply-connected open surfaces. We begin the algorithm by obtaining an initial planar parameterization via double covering and spherical conformal mapping. Note that even the size of the surface is doubled by double covering, the combination of the double covering technique and the spherical conformal mapping results in an efficient computation because of the symmetry. After that, we normalize the boundary and compose the map with a quasi-conformal map so as to correct the conformality distortion and achieve the bijectivity. Our proposed formulation is entirely linear, and hence the computation is significantly accelerated by over 60% when compared with the fastest state-of-the-art approaches. At the same time, our parameterization results are of comparable quality to those produced by the other state-of-the-art approaches in terms of the conformality distortions, the bijectivity and the robustness. Therefore, our proposed algorithm is highly practical in real applications, especially for the problems for which the computational complexity is the main concern.

Note that there is a normalization step in Step 5 of Algorithm 2 for getting a circular boundary. In Step 7 of Algorithm 2, we compose the normalized parameterization map with another quasi-conformal map. By Theorem 4.4, the composition helps improving the conformality of the interior of the disk parameterization. The boundary condition can be further improved for achieving better conformality if we can optimally allocate the boundary vertices on the unit circle. However, previous approaches on this issue are nonlinear and hence incorporating them into our current algorithm will significantly decrease the efficiency of it. In the future, we plan to develop a linear approach for tackling this problem. We will also explore more applications, such as remeshing and registration of simply-connected open surfaces, based on the proposed parameterization scheme.

Acknowledgment Lok Ming Lui is supported by RGC GRF (Project ID: 404612).

References

1. Angenent, S., Haker, S., Tannenbaum, A., Kikinis, R.: Conformal geometry and brain flattening. In: Medical Image Computing and Computer-Assisted Intervention (MICCAI), pp. 271–278 (1999)
2. Bates, P.W., Wei, G.W., Zhao, S.: Minimal molecular surfaces and their applications. J. Comput. Chem. **29**(3), 380–391 (2008)
3. Choi, P.T., Lam, K.C., Lui, L.M.: FLASH: Fast Landmark aligned spherical harmonic parameterization for genus-0 closed brain surfaces. SIAM J. Imag. Sci. **8**(1), 67–94 (2015)
4. Choi, P.T., Lui, L.M.: Fast disk conformal parameterization of simply-connected open surfaces. J. Sci. Comput. **65**(3), 1065–1090 (2015)
5. Desbrun, M., Meyer, M., Alliez, P.: Intrinsic parameterizations of surface meshes. Comput. Graph. Forum **21**(3), 209–218 (2002)
6. do Carmo, M.: Differential Geometry of Curves and Surfaces. Prentice Hall (1976)
7. Feng, X., Xia, K., Tong, Y., Wei, G.W.: Geometric modeling of subcellular structures, organelles, and multiprotein complexes. Int. J. Numer. Methods Biomed. Eng. **28**(12), 1198–1223 (2012)
8. Floater, M.: Parameterization and smooth approximation of surface triangulations. Comput. Aided Geom. Des. **14**(3), 231–250 (1997)

9. Floater, M.: Mean value coordinates. Comput. Aided Geom. Des. **20**(1), 19–27 (2003)
10. Floater, M., Hormann, K.: Parameterization of triangulations and unorganized points. In: Tutorials on multiresolution in geometric modelling, pp. 287–316 (2002)
11. Floater, M., Hormann, K.: Surface parameterization: a tutorial and survey. In: Advances in Multiresolution for Geometric Modelling, oo. 157–186 (2005)
12. Gardiner, F., Lakic, N.: Quasiconformal Teichmüller Theory. American Mathematics Society (2000)
13. Gotsman, C., Gu, X., Sheffer, A.: Fundamentals of spherical parameterization for 3D meshes. ACM Trans. Graph. (Proc. ACM SIGGRAPH 2003) **22**(3), 358–363 (2003)
14. Gu, X., Yau, S.T.: Computing conformal structures of surfaces. Commun. Inf. Syst. **2**(2), 121–146 (2002)
15. Gu, X., Yau, S.T.: Global conformal surface parameterization. In: Eurographics Symposium on Geometry Processing, pp. 127–137 (2003)
16. Gu, X., Wang, Y., Chan, T.F., Thompson, P.M., Yau, S.-T.: Genus zero surface conformal mapping and its application to brain surface mapping. IEEE Trans. Med. Imag. **23**(8), 949–958 (2004)
17. Haker, S., Angenent, S., Tannenbaum, A., Kikinis, R., Sapiro, G.: Conformal surface parameterization for texture mapping. IEEE Trans. Vis. Comput. Graph. **6**(2), 181–189 (2000)
18. Hormann, K., Greiner, G.: MIPS: An efficient global parametrization method. Curve Surf. Des. 153–162 (2000)
19. Hormann, K., Labsik, U., Greiner, G.: Remeshing triangulated surfaces with optimal parameterizations. Comput. Aided Des. **33**(11), 779–788 (2001)
20. Hormann, K., Lévy, B., Sheffer, A.: Mesh parameterization: Theory and practice. SIGGRAPH 2007 Course Notes **2**, 1–122 (2007)
21. Jin, M., Wang, Y., Gu, X., Yau, S.T.: Optimal global conformal surface parameterization for visualization. Commun. Inf. Syst. **4**(2), 117–134 (2005)
22. Jin, M., Kim, J., Luo, F., Gu, X.: Discrete surface Ricci flow. IEEE Trans. Vis. Comput. Graph. **14**(5), 1030–1043 (2008)
23. Jost, J.: Riemannian Geometry and Geometric Analysis. Universitext, Springer (2011)
24. Kharevych, L., Springborn, B., Schröder, P.: Discrete conformal mappings via circle patterns. ACM Trans. Graph. **25**(2), 412–438 (2006)
25. Lévy, B., Petitjean, S., Ray, N., Maillot, J.: Least squares conformal maps for automatic texture atlas generation. ACM Trans. Graph. (Proc. ACM SIGGRAPH 2002) **21**(3), 362–371 (2002)
26. Wang, Y., Lui, L.M., Chan, T.F., Thompson, P.M.: Optimization of Brain Conformal Mapping with Landmarks, Medical Image Computing and Computer Assisted Intervention(MICCAI), Part II, pp. 675–683 (2005)
27. Wang, Y., Lui, L.M., Gu, X., Hayashi, K.M., Chan, T.F., Thompson, P.M., Yau, S.-T.: Brain surface conformal parameterization using Riemann surface structure. IEEE Trans. Med. Imag. **26**(6), 513–538 (2007)
28. Wang, Y., Lui, L.M., Chan, T.F., Thompson, P.M.: Landmark constrained genus zero surface conformal mapping and its application to brain mapping research. Appl. Numer. Math. **57**, 847–858 (2007)
29. Lui, L.M., Wong, T.W., Zeng, W., Gu, X.F., Thompson, P.M., Chan, T.F., Yau, S.T.: Optimization of surface registrations using Beltrami holomorphic flow. J. Sci. Comput. **50**(3), 557–585 (2012)
30. Lui, L.M., Gu, X., Chan, T.F., Yau, S.-T.: Variational method on Riemann surfaces using conformal parameterization and its applications to image processing. J. Methods Appl. Anal. **15**(4), 513–538 (2008)
31. Lui, L.M., Thiruvenkadam, S., Wang, Y., Thompson, P., Chan, T.F.: Optimized conformal surface registration with shape-based landmark matching. SIAM J. Imag. Sci. **3**(1), 52–78 (2010)
32. Lui, L.M., Wong, T.W., Gu, X.F., Thompson, P.M., Chan, T.F., Yau, S.T.: Shape-based diffeomorphic registration on hippocampal surfaces using Beltrami holomorphic flow. Medical Image Computing and Computer Assisted Intervention(MICCAI), Part II, LNCS 6362, pp. 323-330 (2010)
33. Lui, L.M., Lam, K.C., Wong, T.W., Gu, X.: Texture map and video compression using beltrami representation. SIAM J. Imag. Sci. **6**(4), 1880–1902 (2013)
34. Lui, L.M., Zeng, W., Yau, S.T., Gu, X.F.: Shape analysis of planar multiply-connected objects using conformal welding. IEEE Trans. Pattern Anal. Mach. Intell. **36**(7), 1384–1401 (2013)
35. Lai, R., Wen, Z., Yin, W., Gu, X.F., Lui, L.M.: Folding-Free global conformal mapping for genus-0 surfaces by harmonic energy minimization. J. Sci. Comput. **58**(3), 705–725 (2013)

36. Lam, K.C., Lui, L.M.: Landmark and intensity based registration with large deformations via quasi-conformal maps. SIAM J. Imag. Sci. **7**(4), 2364–2392 (2014)
37. Wen, C.F., Lui, L.M.: Geometric registration of high-genus surfaces. SIAM J. Imag. Sci. **7**(1), 337V365 (2014)
38. Ng, T.C., Lui, L.M.: A splitting method for diffeomorphism optimization problem using Beltrami coefficients. J. Sci. Comput **63**(2), 573–611 (2015)
39. Luo, F.: Combinatorial yamabe flow on surfaces. Commun. Contemp. Math. **6**(5), 765–780 (2004)
40. Mullen, P., Tong, Y., Alliez, P., Desbrun, M.: Spectral conformal parameterization. Comput. Graph. Forum **27**(5), 1487–1494 (2008)
41. Pinkall, U., Polthier, K.: Computing discrete minimal surfaces and their conjugates. Exp. Math. **2**(1), 15–36 (1993)
42. Praun, E., Hoppe, H.: Spherical parametrization and remeshing. ACM Trans. Graph. (Proc. ACM SIGGRAPH 2003) **22**(3), 340–349 (2003)
43. Remacle, J.-F., Geuzaine, C., Compère, G., Marchandise, E.: High quality surface remeshing using harmonic maps. Int. J. Numer. Methods Eng. **83**(4), 403–425 (2010)
44. Schoen, R., Yau, S.T.: Lectures on Differential Geometry. International Press (1994)
45. Schoen, R., Yau, S.: Lectures on Harmonic Maps. International Press (1997)
46. Sharon, E., Mumford, D.: 2D-shape analysis using conformal mapping. Int. J. Comput. Vis. **70**(1), 55–75 (2006)
47. Sheffer, A., de Sturler, E.: Surface parameterization for meshing by triangulation flattening. In: Proceedings of 9th International Meshing Roundtable, pp. 161–172 (2000)
48. Sheffer, A., Lévy, B., Mogilnitsky, M., Bogomyakov, A.: ABF++: Fast And robust angle based flattening. ACM Trans. Graph. **24**(2), 311–330 (2005)
49. Sheffer, A., Praun, E., Rose, K.: Mesh parameterization methods and their applications. Found. Trends Comput. Graph. Vis. **2**(2), 105–171 (2006)
50. Yang, Y.L., Guo, R., Luo, F., Hu, S.M., Gu, X.F.: Generalized discrete Ricci flow. Comput. Graph. Forum **28**(7), 2005–2014 (2009)
51. Zhang, E., Mischaikow, K., Turk, G.: Feature-based surface parameterization and texture mapping. ACM Trans. Graph. **24**(1), 1–27 (2005)
52. AIM@SHAPE Shape Repository. http://shapes.aim-at-shape.net/
53. Stanford 3D Scanning Repository. http://graphics.stanford.edu/data/3Dscanrep/
54. A Benchmark for 3D Mesh Segmentation. http://segeval.cs.princeton.edu/
55. RiemannMapper: A Mesh Parameterization Toolkit. http://www3.cs.stonybrook.edu/~gu/software/RiemannMapper/